Contrib Mineral Petrol (2005) 148: 735–745
DOI 10.1007/s00410-004-0636-5

ORIGINAL PAPER

Tammie L. Gerke · Attila I. Kilinc · Richard O. Sack

Ti-content of high-Ca pyroxenes as a petrogenetic indicator: an experimental study of Mafic Alkaline Rocks from the Mt. Erebus volcanic region, Antarctica

Received: 22 January 2004 / Accepted: 22 October 2004 / Published online: 19 November 2004

Abstract We report chemical and mineralogical data for one atmosphere melting experiments conducted on alkalic rocks from the Mt. Erebus volcanic region: DVDP2 basanite, two hawaiites (DVDP2 and a nepheline-bearing variety), and an anorthoclase phonolite. Temperatures between 1,224 and 1,049°C were investigated at f_{O2}~QFM. DVDP2 basanite appears to be an intermediate pressure liquid or a cumulate, because only olivine coexists with melt from above 1,224–1,160°C. High-Ca pyroxene joins olivine in the crystallization sequence at 1,138°C. These minerals are joined by plagioclase at a temperature between 1,120 and 1,104°C. In contrast, DVDP2 hawaiite appears to be relatively evolved, because it is multiply saturated with olivine, plagioclase, and high-Ca pyroxene near its liquidus (between 1,120 and 1,104°C). Plagioclase crystallizes in the Ne-hawaiite by 1,160°C followed by olivine below 1,120°C. The liquidus of anorthoclase phonolite is between the lowest temperatures investigated, 1,089 and 1,049°C, and plagioclase is the liquidus mineral. Our results indicate that DVDP2 hawaiite can be derived from a DVDP2 basanitic parental magma by crystal fractionation at low pressures, that the nepheline hawaiite is an olivine cumulate, and that the liquids parental to the anorthoclase phonolite represent the end products of crystal fractionation. They also allow us to illustrate how the Ti-content of pyroxene may be used as a petrogenetic indicator of processes and events in the evolution of the Erebus volcanic system.

Editorial Responsibility: T. L. Grove

T. L. Gerke (✉) · A. I. Kilinc
Department of Geology,
University of Cincinnati, Cincinnati,
OH USA, 45221-0013
E-mail: erebus@choice.net
Tel.: +1-513-5563732
Fax: +1-513-5566931

R. O. Sack
OFM Research, 28430 NE 47th Place,
Redmond, WA USA, 98053-8841

Introduction

The study of alkalic rocks provides insights into the mineralogical and chemical characteristics of their source regions, the role of assimilation in the differentiation of their magmas, and relationship of alkalic magmas to other magma types. Numerous experimental studies have focused on the effects of low-pressure differentiation on alkalic systems (Brotzu et al. 1983; Aurisicchio et al. 1983; Mayhood and Baker 1986; Sack et al. 1987; Gee and Sack 1988; Kennedy et al. 1990; Thy 1991; Camur and Kilinc 1995). These studies demonstrate that low-pressure fractionation controls the diversity of many alkalic rocks in continental and oceanic regions. However, in the generation of mafic alkaline rocks, the roles of polybaric fractionation (Sack et al. 1987), and magma mixing (Araña et al. 1994) should not be precluded.

Sack et al. (1987) conducted a series of experiments with silica-undersaturated alkalic rocks at one atmosphere pressure to define the compositional trends in multiple saturated melts. They developed a pseudo-liquidus olivine-clinopyroxene-nepheline ternary diagram and projected the position of the one atmosphere cotectic onto the diagram from the plagioclase apex (Sack et al. 1987, Fig. 12). Using data from the literature, they also superimposed the position of the 8–30 Kb pressure cotectic onto the same diagram. Using the pseudo-liquidus olivine-clinopyroxene-nepheline ternary diagram they interpreted the evolution of alkalic rocks from different tectonic environments. Plots of bulk compositions of natural alkalic rocks from continental and oceanic regions on their pseudo-liquidus ternary diagram show that the compositional spectrum of these rocks is compatible with differentiation of their magmas at low pressures (Sack et al. 1987, Fig. 16a–d).

Mt. Erebus, the southern most active volcano in the world, is located on the southern extension of the Terror Rift (Kyle 1990) on Ross Island, Antarctica. Using data

from Moore (1986) and Kyle (1976), geochemical variation diagrams were generated to determine if the basanites, hawaiites, benmoreites, mugearites, and phonolites of the Mt. Erebus volcanic region are genetically related (Fig. 1 a–g). The continuous data arrays in Fig. 1 a–g are consistent with the basanite, hawaiite, and phonolite being part of the same differentiation series.

In order to assess the importance of low-pressure differentiation in the petrogenesis of mafic alkaline rocks from the Mt. Erebus volcanic region, Antarctica, we conducted a series of experiments with a suite of rocks from this region at one atmosphere pressure and at f_{O2}~QFM. The objectives of this study are to (1) provide the first set of low pressure experimental data for the mafic alkalic rocks from the Mt. Erebus region, Antarctica, (2) test the hypothesis that the DVDP2 hawaiite is the low pressure fractionation product of the DVDP2 basanite magma, and (3) examine the systematics of the Ti-content of high-calcium clinopyroxenes in equilibrium with mafic alkaline melts to determine if it can be used as a petrogenetic indicator.

Experimental methods

Starting materials

Starting materials for the experiments were the Dry Valley Drilling Project 2 (DVDP2) basanite, two hawaiites (DVDP2 hawaiite and Tent Island 83415 Ne-hawaiite), and Mt. Erebus anorthoclase phonolite (Table 1). Major mineralogy of the DVDP2 basanite is olivine (Fo_{74}–Fo_{87}), high-calcium pyroxene (En_{39}–En_{43}), plagioclase (An_{62}–An_{72}), apatite, and opaques. The DVDP2 hawaiite is a vesicular basalt composed of olivine (Fo_{85}), high-calcium pyroxene (En_{30}–En_{41}), kaersutite, plagioclase (An_3–An_{57}), apatite, and opaques. The 83415 Ne-hawaiite is a porphyritic alkaline basalt composed of olivine (Fo_{65}–Fo_{84}), high-calcium pyroxene (En_{36}–En_{38}), plagioclase (An_{40}–An_{51}), apatite, and opaques. The anorthoclase phonolite is a vesicular porphyritic alkaline basalt composed of olivine (Fo_{46}–Fo_{57}), high-calcium pyroxene (En_{34}–En_{41}), anorthoclase (An_6–An_{26}), apatite, and opaques. For additional descriptions of rocks see Moore (1986) and Kyle (1976, 1977, 1981). Representative analyses of major minerals in the DVDP2 basanite, DVDP2 hawaiite, 83415 Ne- hawaiite, and anorthoclase phonolite are given in Table 2.

Table 1 XRF whole rock data for rocks used in experiments

	DVDP2[a] (Basanite)	DVDP2[a] (Hawaiite)	83415[b] (Ne-hawaiite)	83452[b] (Phonolite)
SiO_2	41.68	47.27	49.53	55.00
TiO_2	4.06	2.95	2.12	1.36
Al_2O_3	12.96	17.61	19.87	18.29
Fe_2O_3*	3.06	3.35	0.00	0.00
FeO*	8.48	6.06	7.41	6.59
MnO	0.18	0.21	0.17	0.27
MgO	12.13	3.72	3.00	1.64
CaO	11.32	7.76	6.93	3.34
Na_2O	3.16	6.07	6.22	7.77
K_2O	1.48	3.11	3.00	4.39
P_2O_5	0.84	0.81	0.85	0.56
Total	99.35	98.92	99.10	99.21

[a]Data from Kyle (1981)
[b]Data from Moore (1986)

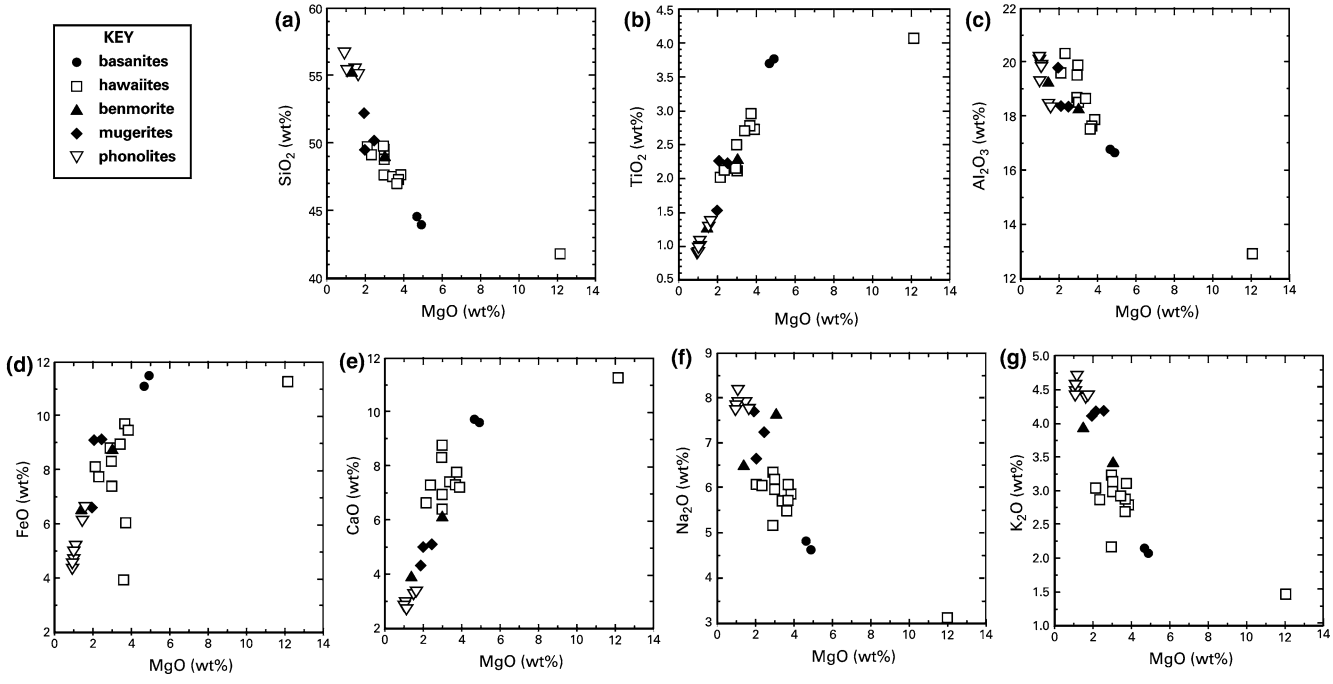

Fig. 1 a–g Geochemical variation diagrams of SiO_2, TiO_2, Al_2O3, FeO, CaO, Na_2O, and K_2O plotted against MgO. XRF data from Kyle (1977) and Moore (1986). *Filled circles* basanites, *filled squares*

Table 2 Average analysis with standard deviations of minerals in the natural rock starting material

	SiO_2	TiO_2	Al_2O_3	FeO*[a]	MnO	MgO	CaO	Na_2O	K_2O	P_2O_5	Total	No. of analysis
DVDP2 Basanite												
Olivine	38.89	0.02	0.07	15.60	0.19	43.20	0.23	0.02	0.00	0.04	98.42	5
	0.57	0.02	0.03	2.96	0.08	2.54	0.04	0.01	0.01	0.03		
Clinopyroxene												
Low Ti	44.67	3.22	9.12	5.73	0.05	12.27	22.36	0.74	0.01	0.01	98.22	3
	0.14	0.03	0.41	0.60	0.04	0.67	0.34	0.31	0.01	0.01		
High Ti	40.12	6.37	11.53	6.77	0.00	10.48	22.90	0.46	0.00	0.02	98.69	1
	0.62	0.07	0.39	0.09	0.02	0.02	0.57	0.34	0.06	0.02		
Plag	50.38	0.21	30.88	0.43	0.01	0.04	13.25	3.75	0.25	0.05	99.24	10
	0.62	0.07	0.39	0.09	0.02	0.02	0.57	0.34	0.06	0.02		
DVDP2 hawaiite												
Olivine	39.54	0.00	0.05	13.44	0.22	44.95	0.16	0.02	0.01	0.04	98.67	2
	0.18	0.00	0.01	0.04	0.07	0.08	0.03	0.02	0.01	0.05		
Clinopyroxene												
Low Ti	47.72	2.35	4.73	7.27	0.20	12.98	22.37	0.54	0.01	0.05	98.21	4
	0.35	0.14	0.21	0.13	0.02	0.10	0.06	0.02	0.01	0.04		
High Ti	43.86	3.32	8.94	8.65	0.23	10.39	21.82	0.83	0.00	0.05	98.09	4
	0.50	0.41	0.39	0.96	0.06	0.76	0.48	0.21	0.01	0.02		
Plag	56.08	0.17	27.76	0.56	0.03	0.09	9.08	5.90	0.61	0.06	100.36	9
	3.06	0.05	1.53	0.12	0.03	0.05	2.06	0.91	0.34	0.06		
83415 Ne-hawaiite												
Olivine	37.19	0.07	0.06	26.58	0.74	33.67	0.40	0.05	0.01	0.10	98.86	4
	0.25	0.02	0.02	1.52	0.12	1.29	0.03	0.01	0.01	0.03		
Clinopyroxene	47.07	2.77	5.96	7.62	0.26	11.82	21.59	0.94	0.00	0.03	98.10	4
	0.81	0.45	0.66	0.07	0.03	0.42	0.23	0.06	0.01	0.02		
Plag	55.99	0.15	27.78	0.29	0.02	0.06	9.31	5.56	0.77	0.03	99.96	7
	1.09	0.05	0.69	0.08	0.03	0.02	0.81	0.36	0.14	0.02		
Anorthoclase phonolite												
Olivine	33.77	0.03	0.03	40.78	2.58	21.11	0.53	0.03	0.00	0.05	98.93	12
	0.51	0.03	0.02	1.87	0.19	1.76	0.06	0.02	0.00	0.02		
Clinopyroxene												
Low Ti	49.77	1.44	3.10	9.96	0.61	12.05	20.80	0.96	0.01	0.05	98.75	5
	0.91	0.42	0.85	1.26	0.20	0.86	0.30	0.21	0.01	0.04		
High Ti	44.11	3.90	8.36	8.87	0.29	11.20	20.71	0.85	0.01	0.04	98.34	7
	1.34	0.45	1.22	0.39	0.10	0.18	0.18	0.18	0.01	0.03		
Plag	62.50	0.24	21.53	0.91	0.05	0.13	2.63	6.98	3.67	0.06	98.72	8
	2.62	0.41	0.95	2.03	0.11	0.30	0.58	1.38	0.71	0.12		

[a]FeO* = Total iron

Experimental conditions

Each sample was ground to a particle size of 5–10 microns and then 5–6 g of rock powder was mixed with polyvinyl alcohol and pressed into 10 mm diameter pellets. A small hole was drilled in a portion of each pellet and the sample was hung on a Fe-electroplated platinum wire (0.127 mm in diameter). Pt wires were electroplated in a ferrous ammonium sulfate-ferrous sulfate solution. They were then annealed in a 95.25% CO_2 and 4.75% CO mixture in a vertical Deltech one-atmosphere gas-mixing furnace for 72 h at 1,200°C to minimize the loss of iron from the samples. Samples were hung on a Pt-basket placed in the furnace. A Mode C controller (Deltech Inc.) controlled the furnace temperature and temperatures were measured using a Pt–Pt–10% Rh thermocouple. Temperature readings are accurate to ±2°C. Oxygen fugacity was controlled using a 95.25% CO_2 and 4.75% CO mixture corresponding approximately to the Quartz-Fayalite-Magnetite (QFM) buffer at 1,200°C. The flow rates of CO and CO_2 were controlled using a Matheson, Inc., flow meter. Samples were quenched by dropping the Pt-wire basket into cold distilled-deionized water. One-atmosphere experiments were conducted at temperatures between 1,224 and 1,049°C with average intervals of approximately 22°. The duration of experiments ranged from 96 to 1,000 h.

Analytical procedure

Chemical compositions of the glasses and coexisting minerals were determined using a four-channel Cameca SX-50 electron microprobe at Purdue University. The accelerating voltage was 15 kV and beam current was 0.15×10^{-7} amps. Beam size for all of the analyses was 1 micron. The beam was continuously and rapidly moved during analysis of Na_2O to reduce the alkali loss from the glasses. The microprobe standards used by Sack et al. (1987) were used in this study. Correction procedures were those given by Bence and Albee (1968) and Albee and Ray (1970). Reported microprobe analyses are accurate within ±20% of the amount present

for Na_2O and K_2O and ±3% of the amount present for the other oxides.

FeO loss from the sample is minimized by the annealing process of the Pt-wire however, there is little that can be done to minimize the loss of Na_2O while a sample is in the furnace. The extent of Na_2O and FeO loss from the starting material was calculated by multiple regression (Table 3). These were conducted by regressing either Na_2O or FeO against the bulk composition, the glass composition, and mineral phase(s) at a given temperature. Temperatures, log f_{O2}, duration of experiments, and run products are also presented in Table 3. For the DVDP2 hawaiite Run no. 17 no high-Ca pyroxene was detected in the microprobe analyses but based on the multiple regression analysis there should have been approximately 13 wt%. For the 83415 Ne-hawaiite Run no.13 no plagioclase was detected in the microprobe analyses however based on the glass phase wt% there should be approximately 4 wt% plagioclase. Table 4 lists the compositions of the run products determined by microprobe analysis.

Attainment of equilibrium

One approach to determine if equilibrium or near equilibrium conditions have been achieved is to compare the calculated K_D for Fe^{2+}–Mg^{2+} exchange between olivine and coexisting melt in the experimental charges and compare it with the predicted K_D value(s). Roeder and Emslie (1970) and Ringwood (1975) indicated that the K_D value for Fe^{2+}–Mg^{2+} exchange between olivine and coexisting melt is 0.3 ± 0.03. However there is a significant amount of experimental data indicating that K_D values may be substantially different from 0.3 for compositions outside the tholeiitic range (Smith 1992; Sack et al. 1987; Gee and Sack 1988; Gerke and Kilinc 1993; Gerke 1995; Camur and Kilinc 1995; Kilinc and Gerke 2003).

Table 3 Phase assemblages of the one atmosphere experiments

Run no.	T (°C)	Log fO_2	Duration (h)	Run products	Phase propotions (wt%)				Loss (wt%)	
					gl	ol	cpx	pl	Na_2O	FeO
DVDP2 basanite										
11	1,224	−8.12	96	gl, ol	90.70	8.30			0.93	
8	1,197	−8.38	120	gl, ol	89.70	10.00			0.84	
9	1,177	−8.66	120	gl, ol	86.60	13.40			0.50	
10	1,160	−8.94	168	gl, ol	85.10	15.10			0.51	
12	1,138	−9.23	360	gl, ol, cpx	78.20	15.30	5.50		0.82	
13	1,120	−9.53	360	gl, ol, cpx, op	69.80	15.20	13.70		1.17	
15	1,104	−9.83	264	gl, ol, cpx, pl, op	42.20	18.60	23.90	13.10	0.60	
DVDP2 hawaiite										
11	1,224	−8.12	96	gl	97.90				1.30	
8	1,197	−8.38	120	gl	99.60				0.68	
9	1,177	−8.66	120	gl	99.80				0.56	
10	1,160	−8.94	168	gl	99.60				0.68	
12	1,138	−9.23	360	gl	98.62				0.90	
13	1,120	−9.53	360	gl	97.70				1.47	
15	1,104	−9.83	264	gl, pl, ol, cpx	93.60	1.14	5.39	0.58	0.42	
17	1,089	−9.93	840	gl, pl, ol	82.50	2.61	12.86	0.79	0.90	
16	1,049	−10.64	1,000	gl, pl, ol, cpx, op	61.40	2.97	22.81	8.21	1.08	
83415 Ne-hawaiite										
11	1,224	−8.12	96	gl	98.20				0.73	0.94
8	1,197	−8.38	120	gl	99.20				0.64	1.05
9	1,177	−8.66	120	gl	100.00				0.40	0.50
10	1,160	−8.94	168	gl, pl	97.50			1.33	0.87	0.36
12	1,138	−9.23	360	gl, pl	91.10			8.07	0.47	0.31
13	1,120	−9.53	360	gl	96.20				1.41	0.88
15	1,104	−9.83	264	gl, pl, ol	75.30	1.85		21.40	0.98	1.34
17	1,089	−9.93	840	gl, pl, ol, op	69.80	2.58		27.04	0.99	0.06
16	1,049	−10.64	1000	gl, pl, ol, op	60.20	3.89		34.34	0.78	1.27
Anorthoclase phonolite										
9	1,177	−8.66	120	gl	97.81				0.78	1.13
10	1,160	−8.94	168	gl	97.67				0.81	1.03
12	1,138	−9.23	360	gl	96.87				1.16	1.21
13	1,120	−9.53	360	gl	97.58				1.21	0.93
15	1,104	−9.83	264	gl	98.71				0.56	1.14
17	1,089	−9.93	840	gl	98.60				0.91	0.86
16	1,049	−10.64	1,000	gl, pl	93.05			5.64	0.91	0.49

gl glass, *ol* olivine, *cpx* clinopyroxen, *pl* plagioclase, *op* opaques

Table 4 Electron microprobe analyses of run products

Sample	Run no.	Phase	SiO_2	TiO_2	Al_2O_3	Fe_2O_3[a]	FeO[a]	MnO	MgO	CaO	Na_2O	K_2O	P_2O_5	Total
Basanite	11	gl	42.49	4.75	13.94	1.60	8.84	0.18	9.02	12.26	2.46	1.26	0.74	97.54
		ol	39.44	0.06	0.11	0.00	12.54	0.18	45.86	0.49	0.02	0.01	0.05	98.76
	8	gl	42.16	4.72	14.06	1.68	8.79	0.13	8.36	12.60	2.59	1.34	0.79	97.22
		ol	39.90	0.05	0.08	0.00	13.45	0.20	45.41	0.53	0.02	0.02	0.04	99.69
	9	gl	42.05	5.03	14.79	1.65	8.42	0.16	7.09	12.88	3.07	1.50	0.91	97.55
		ol	39.79	0.07	0.08	0.00	14.27	0.22	44.38	0.57	0.02	0.01	0.03	99.44
	10	gl	42.12	5.07	15.07	1.58	8.21	0.22	6.49	13.15	3.11	1.51	0.92	97.43
		ol	39.12	0.04	0.08	0.00	15.26	0.22	43.26	0.54	0.02	0.01	0.03	98.58
	12	gl	42.62	5.18	15.82	1.54	8.38	0.16	6.12	12.68	2.96	1.52	0.99	97.96
		ol	39.14	0.07	0.07	0.00	16.00	0.26	43.32	0.58	0.02	0.00	0.03	99.48
		cpx	43.31	4.68	9.62	0.00	4.90	0.04	12.21	22.84	0.35	0.00	0.01	97.94
	13	gl	43.04	5.31	16.40	1.46	8.75	0.18	5.67	11.67	2.76	1.33	0.59	97.15
		ol	38.16	0.12	0.08	0.00	18.11	0.27	41.36	0.46	0.01	0.00	0.05	98.61
		cpx	44.11	3.86	8.91	0.00	5.74	0.08	12.56	21.32	0.42	0.07	0.05	97.11
	15	gl	42.64	5.39	15.92	1.67	8.32	0.19	4.23	9.48	4.82	2.76	1.87	97.26
		ol	37.95	0.09	0.07	0.00	21.34	0.33	38.19	0.56	0.01	0.01	0.02	98.55
		cpx	43.99	4.68	8.15	0.00	6.66	0.14	12.03	22.11	0.53	0.03	0.10	98.40
		pl	48.75	0.74	29.70	0.00	1.27	0.03	0.44	13.39	3.37	0.58	0.16	98.40
DVDP2 hawaiite	11	gl	48.31	3.15	18.04	1.45	7.23	0.22	3.83	7.92	4.86	2.62	0.35	97.97
	8	gl	47.44	3.27	17.80	1.60	7.31	0.18	3.76	7.82	5.41	2.72	0.55	97.83
	9	gl	47.33	3.17	17.73	1.57	7.24	0.20	3.82	7.77	5.52	2.81	0.68	97.81
	10	gl	47.41	3.11	17.85	1.47	7.17	0.19	3.78	7.67	5.41	2.82	0.65	97.54
	12	gl	47.81	3.34	18.16	1.45	7.26	0.23	3.83	7.84	5.24	2.86	0.65	98.67
	13	gl	48.33	3.10	18.15	1.27	6.99	0.25	3.88	8.01	4.71	2.54	0.20	97.44
	15	gl	46.80	3.36	17.14	1.52	7.52	0.21	3.45	7.44	5.80	3.07	0.79	97.08
		ol	36.97	0.10	0.07	0.00	23.20	0.57	36.65	0.52	0.04	0.02	0.19	98.30
		cpx	46.56	2.83	5.44	0.00	7.45	0.20	12.63	21.74	0.62	0.03	0.09	97.56
		pl	51.74	0.20	29.04	0.00	0.57	0.00	0.13	11.91	4.12	0.50	0.06	98.27
	17	gl	47.63	3.83	16.67	1.70	8.07	0.19	3.29	7.19	5.62	3.23	0.67	98.08
		ol	38.23	0.16	1.17	0.00	24.18	0.57	33.09	0.85	0.23	0.05	0.06	98.59
		pl	51.73	0.19	29.42	0.00	0.66	0.02	0.14	12.23	4.05	0.49	0.06	98.98
	16	gl	49.39	3.29	17.36	1.35	6.76	0.23	2.41	5.78	6.16	3.91	1.22	97.83
		ol	37.47	0.41	1.35	0.00	26.94	0.79	29.92	0.93	0.43	0.28	0.14	98.66
		cpx	46.75	3.15	5.83	0.00	7.52	0.22	12.20	21.69	0.61	0.06	0.07	98.09
		pl	53.56	0.66	26.70	0.00	1.82	0.05	0.46	9.79	5.02	1.19	0.21	99.46
83415 Ne-hawaiite	11	gl	50.19	2.33	20.78	1.12	5.58	0.11	2.93	7.16	5.59	2.79	0.55	99.12
	8	gl	49.76	2.37	20.41	1.10	5.42	0.16	2.84	7.06	5.62	2.69	0.46	97.89
	9	gl	49.35	2.37	20.21	1.19	5.84	0.18	2.88	6.95	5.82	2.79	0.64	98.22
	10	gl	50.00	2.63	20.14	1.17	6.17	0.18	3.16	6.80	5.43	2.93	0.79	99.40
		pl	51.51	0.22	30.25	0.00	0.54	0.01	0.15	12.61	3.78	0.42	0.06	99.56
	12	gl	49.72	2.83	19.35	1.32	6.58	0.20	3.30	6.33	5.95	3.18	0.71	99.49
		pl	51.60	0.25	30.15	0.00	0.31	0.01	0.02	12.40	4.08	0.39	0.04	99.21
	13	gl	51.43	2.29	21.02	1.00	5.89	0.15	3.03	6.96	5.00	2.67	0.28	99.69
	15	gl	49.61	2.88	18.52	1.19	6.42	0.22	2.99	5.77	5.59	3.62	0.97	97.78
		ol	38.12	0.11	0.14	0.00	19.41	0.40	39.50	0.41	0.03	0.00	0.08	98.18
		pl	53.67	0.17	28.31	0.00	0.36	0.00	0.11	10.50	4.82	0.59	0.01	98.52
	17	gl	48.72	3.10	17.57	1.60	7.96	0.21	2.97	5.71	5.53	3.60	1.20	98.15
		ol	36.16	0.03	0.08	0.00	26.91	0.61	33.16	0.39	0.05	0.00	0.06	97.44
		pl	54.11	0.19	28.03	0.00	0.33	0.00	0.08	10.21	5.07	0.67	0.03	98.72
	16	gl	48.70	3.25	16.97	1.37	6.90	0.29	2.59	5.67	6.04	3.71	1.52	96.99
		ol	36.41	0.07	0.06	0.00	27.56	0.77	32.22	0.45	0.04	0.00	0.05	97.64
		pl	55.20	0.16	27.52	0.00	0.52	0.00	0.06	9.51	5.26	0.78	0.04	99.03
Anortho-phonolite clase	9	gl	55.96	1.53	19.56	1.02	4.66	0.29	1.42	3.34	7.15	4.17	0.27	99.37
	10	gl	56.07	1.48	19.52	1.01	4.78	0.28	1.41	3.38	7.13	4.19	0.35	99.61
	12	gl	56.55	1.55	19.65	0.95	4.70	0.27	1.42	3.33	6.82	4.14	0.24	99.63
	13	gl	56.09	1.44	19.65	0.96	4.94	0.26	1.45	3.43	6.72	3.96	0.24	99.11
	15	gl	55.44	1.48	19.40	0.93	4.68	0.27	1.45	3.25	7.30	4.24	0.49	98.94
	17	gl	55.58	1.42	19.24	0.99	4.92	0.28	1.41	3.29	6.96	4.11	0.32	98.51
	16	gl	55.56	1.61	18.19	1.05	5.58	0.36	1.64	2.87	6.97	4.40	0.45	98.69
		pl	58.80	0.17	25.14	0.00	0.54	0.04	0.09	6.72	6.56	1.26	0.03	99.35

gl glass, *ol* olivine, *cpx* clinopyroxen, *pl* plagioclase
[a]FeO and Fe_2O_3 determined using method given by Kilinc et al. 1983

Using available experimental data Kilinc and Gerke (2003) calculated K_D's of olivine-melt pairs for compositions ranging from alkaline basalt to rhyolite (Camur 1989; Gee and Sack 1988; Gerke and Kilinc 1993; Gerke 1995; Grover and Juster 1989; Grove et al. 1982; Sack et al. 1987; Smith 1992; Ussler and Glazner 1989;

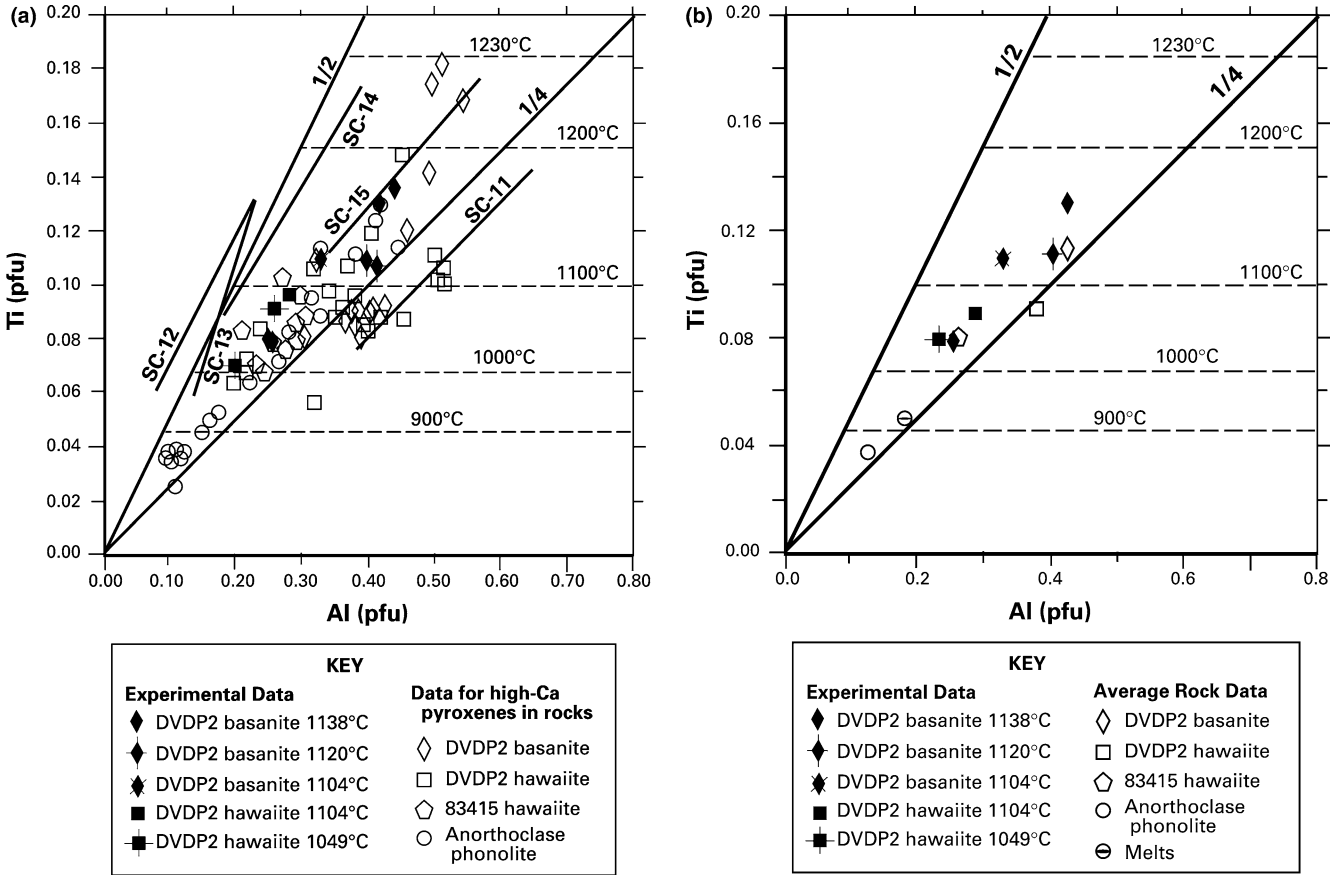

Fig. 2 **a**, **b** Ti and Al contents (atoms per four cation–six oxygen formula unit) of Mt. Erebus natural and experimental high-Ca pyroxenes. Diagonal lines labeled with the ratios 1/2 and 1/4. Line segments labeled SC-11, SC-12, SC-13, SC-14, and SC-15 represent the range of Ti and Al contents in compositionally zoned clinopyroxenes reported by Sack and Carmichael (1984) for one atmosphere (QFM) melting and crystallization experiments at 1,149°C. Horizontal dashed lines indicate the Ti content of the low-Ti pyroxene coexisting with high-Ti high-Ca pyroxene in the $CaMgSi_2O_6$-$CaMg_{0.5}Ti_{0.5}AlSiO_6$ system at 1,230, 1,200, 1,100, 1,000, and 900°C calculated using the algorithms of Sack and Ghiorso (1994a)

Walker et al. 1979) and they ranged from 0.17 to 0.68 respectively. They regressed the variation of K_D with composition into the following equation.

$$\ln K_D = 24.748x^3 - 27.701x^2 + 10.027x - 2.4396$$

where $x = S/(S + CA + M)$: $S = SiO_2$–$2Na_2O$–$4K_2O$, $CA = CaO$–$P_2O_5 + K_2O + 3Na_2O + Fe_2O_3 + Al_2O_3$, and $M = MgO + FeO + MnO$. Oxides are in terms of number of moles.

This equation was used to test if equilibrium was reached in our experiments. Average K_D's for DVDP2 basanite (1,224–1,160°C), DVDP2 hawaiite (1,104–1,049°C), and 83415 Ne-hawaiite (1,104–1,049°C) are 0.28 ± 0.03, 0.30 ± 0.03 and 0.28 ± 0.03, respectively. Calculated K_Ds using the above equation are 0.28, 0.27 and 0.28 respectively. Since measured and calculated K_Ds are statistically not different from each other we conclude that Fe–Mg exchange equilibrium between olivine and melt has been reached in our experiments.

Experimental results

Mineral chemistry

Olivine

The fraction of olivine in run products increases with decreasing temperature (Table 3) in experiments with DVDP2 basanite, DVDP2 hawaiite, and 83415 Ne-hawaiite. There is also a compositional shift from magnesium- to iron-rich from the DVDP2 basanite (Fo_{76}–Fo_{87}) to the hawaiites (DVDP2 Fo_{66}–Fo_{74} and 83415 Fo_{68}–Fo_{78}). Mg number of olivines in DVDP2 basanite, DVDP2 hawaiite and the 83415 Ne-hawaiite range from 87 at high temperatures to 66 at low temperatures.

Clinopyroxene

High-Ca pyroxenes of the natural samples have average molar ratios of $Fe^{2+}/(Fe^{2+} + Mg)$ and $Ca/(Ca + Mg + Fe^{2+})$ for the DVDP2 basanite of 0.136 ± 0.034 and 0.541 ± 0.021, and for the DVDP2 hawaiite, 0.187 ± 0.042 and 0.537 ± 0.021 (Fe^{2+} calculated from Fe_T based on four cations and six oxygens per formula unit [pfu]). The high-Ca pyroxenes in 83415 Ne-hawaiite have average $Fe^{2+}/(Fe^{2+} + Mg)$ ratios of 0.215 ± 0.02, which is comparable to those in the

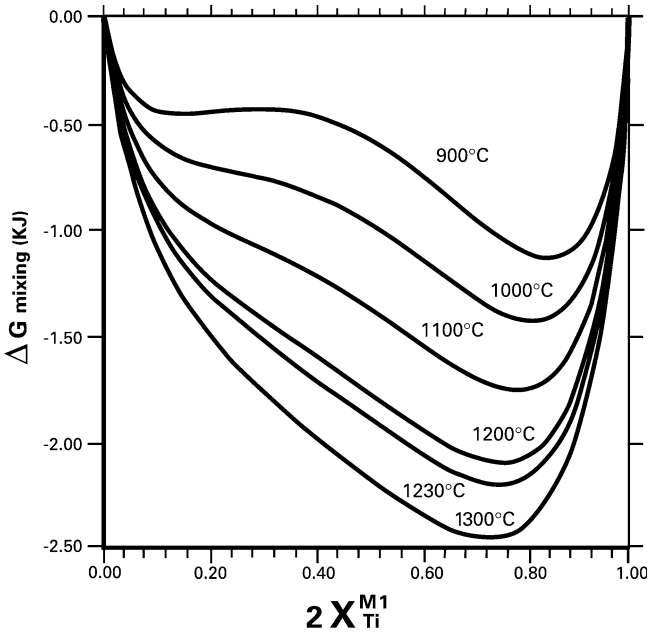

Fig. 3 Molar Gibbs energy of mixing of $CaMgSi_2O_6$-$CaMg_{0.5}Ti_{0.5}AlSiO_6$ pyroxenes at 1,300, 1,230, 1,200, 1,100, 1,000, and 900°C calculated using the algorithms of Sack and Ghiorso (1994a)

DVDP2 hawaiite, and high-Ca pyroxenes in the anorthoclase phonolite have higher average $Fe^{2+}/(Fe^{2+}+Mg)$ ratios, 0.249 ± 0.05, than in the basanite and the hawaiites.

The experimental high-Ca pyroxenes have molar $Fe^{2+}/(Fe^{2+}+Mg)$ and $Ca/(Ca+Fe^{2+}+Mg)$ ratios of 0.129 ± 0.010 and 0.515 ± 0.016 in the DVDP2 basanite, and 0.209 ± 0.029 and 0.499 ± 0.009 in the DVDP2 hawaiite. These ratios compare favorably with the average of these ratios in high-Ca pyroxenes from the rocks.

In addition, high-Ca pyroxenes are enriched in Al, Ti, and Fe^{3+}. These may be characterized by the concentrations of $Ca(Mg, Fe)_{1/2}Ti_{1/2}AlSiO_6$ (alumino-buffonite), $Ca(Mg, Fe)_{1/2}Ti_{1/2}FeSiO_6$ (buffonite), and $CaFeAlSiO_6$ (essenite) components (Sack and Ghiorso 1994a). Experimental and natural Erebus high-Ca pyroxenes are enriched mainly in alumino-buffonite and essenite components, respective ranges of mole fractions of these components being 0.022–0.389 and 0.023–0.227 with mole fractions of buffonite component being small to negligible (−0.001–0.023).

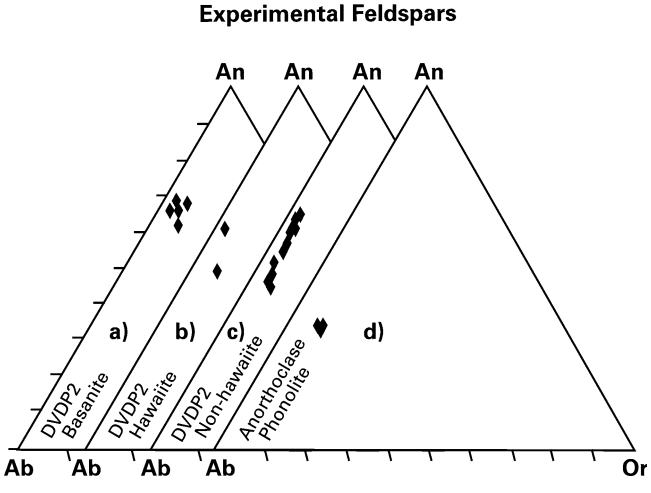

Fig. 4 Ternary diagram for experimental plagioclases from **a** DVDP2 basanite, **b** DVDP2 hawaiite, **c** 83415 Ne-hawaiite, and **d** anorthoclase phonolite

Alternatively, a plot of Ti and Al concentrations (Fig. 2a, b) may be used to illustrate these variations. The Ti concentrations for the high-Ca pyroxenes in the DVDP2 basanite range from ~0.08 to 0.185 pfu, for the DVDP2 hawaiite from ~0.056 to 0.148 pfu, the 83415 Ne-hawaiite ranges from ~0.068 to 0.098 pfu and the anorthoclase phonolite ranges from ~0.03 to 0.13 pfu (Fig. 2a). The two DVDP2 samples and the anorthoclase phonolite all show a large range in Ti concentrations while 83415 Ne-hawaiite has the narrowest range. Also some of the high-Ca pyroxenes from the anorthoclase phonolite have the lowest Ti concentrations observed (~0.03 pfu). All of the high-Ca pyroxenes (natural and experimental) have Ti:Al ratios between 1:2.8 and 1:6 with the majority of the data having Ti:Al ratios between 1:3 and 1:4. Interestingly, high-Ca pyroxenes with two populations of Ti-contents were produced in the experiments on DVDP2 basanite at 1,138°C (Fig.2b). The range of Ti-contents of these high-Ca pyroxenes is similar to, but slightly less than the range of Ti-contents in high-Ca pyroxenes in similar experiments on potash ankaramites (SC- 12–14), leucite nephelinites (SC-15), and melilite nephelinites (SC-11) at 1,149°C (Sack and Carmichael 1984). This may be a result of the shape of the Gibbs free energy of mixing curves for $CaMgSi_2O_6$–$CaMg_{1/2}Ti_{1/2}AlSiO_6$ pyroxenes. The Gibbs free energy of mixing curves are flat between ~Ti 0.14 and 0.3125 pfu at high temperature (Fig. 3) but they take on a more distinct shape as the temperature of the system decreases. For example, at 900°C, a "low-Ti" (0.0465 pfu) and "high-Ti" (0.4075 pfu) high-Ca pyroxene are predicted to coexist (Fig. 3, Sack and Ghiorso 1994a).

Plagioclase

Mineral compositions of the plagioclases (Table 4) coexisting with all four melts are shown in Fig. 4a–d. There is a compositional shift from calcium- to sodium-rich plagioclases in the DVDP2 hawaiite and 83415 Ne-hawaiite with decreasing temperature. Plagioclase only formed in a few experiments with the DVDP2 basanite and anorthoclase phonolite. The compositional range for the DVDP2 basanite (An_{72}–An_{62}) and 83415 Ne-hawaiite (An_{63}–An_{40}) rock and experimental data are similar. The DVDP2 hawaiite (An_{59}–An_{48}) had a smaller compositional range in the experimental data than the rock data (An_{57}–An_3), and the anorthoclase phonolite experimental data was more calcium-rich (An_{33}) than the rock data (An_{26}–An_6). The wider An ranges of the

natural plagioclases appear to reflect crystallization to lower temperatures than those investigated experimentally, and the lower An-content of the natural plagioclases in the anorthoclase phonolite may reflect re-equilibration to lower temperatures.

Melt chemistry

The variation of oxides with MgO in the one-atmosphere melts (Table 4) of the DVDP2 basanite, DVDP2 hawaiite, and 83415 Ne-hawaiite are discussed below. The TiO_2 and K_2O concentrations increase for all three compositions and SiO_2 and Na_2O concentrations increase for DVDP2 basanite and hawaiite with decreasing MgO. This indicates incompatible behavior of these elements with the melt. Al_2O_3 and CaO concentrations decrease in the DVDP2 and 83415 hawaiites but their concentrations initially increase and then decrease in the DVDP2 basanite with decreasing MgO. FeO concentrations vary little in all three compositions and SiO_2 and Na_2O concentrations vary little in the 83415 Ne-hawaiite with decreasing MgO. Based on this the sequence of crystallization for the DVDP2 basanite is olivine followed by clinopyroxene and plagioclase, for DVDP2 hawaiite it is plagioclase followed by olivine and clinopyroxene, and for 83415 Ne-hawaiite it is plagioclase followed by olivine. Because experiments with the anorthoclase phonolites were conducted in the temperature interval of 1,117–1,049°C and only plagioclase formed at the lowest temperature, the sequence of crystallization for anorthoclase phonolites was not determined.

Discussion

Two objectives of this study were to provide the first set of low pressure experimental data for the mafic alkalic rocks from the Mt. Erebus region, Antarctica and to test the hypothesis that the DVDP2 hawaiite is the low pressure fractionation product of the DVDP2 basanite magma. Although both of these rocks are from the same area of the Mt. Erebus volcanic region (Hut Point Peninsula) spatial association does not necessarily indicate a genetic relationship. We have used the following criteria to test this hypothesis. If the DVDP2 hawaiite is the low-pressure differentiation product of the parental DVDP2 basanite then the Mg# of the derivative melt should be identical to the Mg# of the parental melt at the same temperature. Fig. 5 graphically presents the sequence of crystallization for the DVDP2 basanite and the DVDP2 hawaiite. The liquidus temperature of DVDP2 hawaiite is 1,104°C, and at that temperature the Mg# of the melt is 45. The Mg# of the residual melt for DVDP2 basanite at this temperature is also 45. One would expect that both the liquidus mineral assemblage of the DVDP2 hawaiite should be identical to the mineral assemblage for the DVDP2 basanite and that the composition of the mineral phases should be approximately the same. At its liquidus temperature (1,104°C) DVDP2 hawaiite is multiply saturated with olivine, clinopyroxene, and plagioclase. The mineral assemblage for the derivative magma of the DVDP2 basanite at 1,104°C is also olivine, clinopyroxene, and plagioclase. Table 5 compares the compositions of the mineral phases for the DVDP2 basanite and DVDP2 hawaiite at 1,104°C. The high-Ca pyroxenes are more complex because the shape of the Gibbs free energy mixing surface, at this temperature, indicates unmixing will take place (see clinopyroxene discussion). Nevertheless, high-Ca pyroxene compositions are also similar despite the fact that they display a somewhat greater variation in composition between the DVDP2 basanite and DVDP2 hawaiite compared to the olivine and plagioclase. Thus the experimental data are consistent with the inference that the DVDP2 hawaiite is the low-pressure differentiation product of the DVDP basanite.

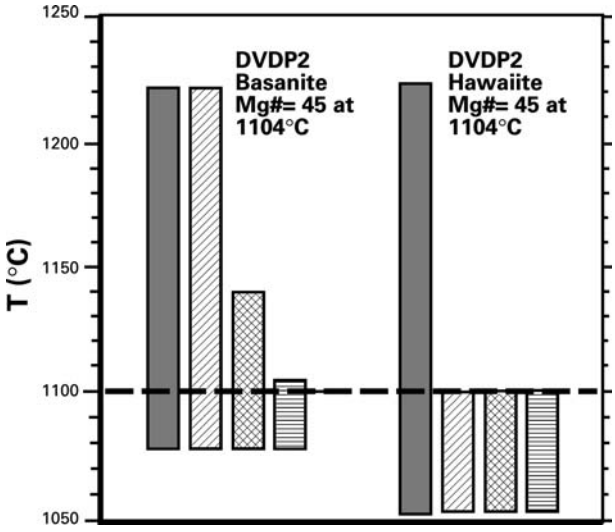

Fig. 5 Experimental sequence of crystallization results for DVDP2 basanite and DVDP2 hawaiite. *Solid bars* melt, *angled pattern* olivine, *hatchered pattern* clinopyroxene, and *weave pattern* plagioclase

Experimental data generated in this study combined with other experiments cited in the literature can be used to determine whether the olivine + high-Ca pyroxene + plagioclase + spinel cotectic (Sack et al. 1987, Fig. 12) is composition dependent. Sack et al. (1987) constrained the position of this cotectic using alkalic rocks from numerous volcanoes. They justified this approach by stating that "major element chemical variations of low-pressure alkaline basalt liquids saturated with olivine, high-calcium pyroxene, and plagioclase may be reduced to a single cotectic curve defined by ratios of olivine/high-calcium pyroxene and olivine/(olivine + high-calcium pyroxene + nepheline) normative components...despite the chemical diversity...." By comparing the positions of other olivine + high-Ca pyroxene + plagioclase + spinel cotectics determined

Table 5 Average mineral compositions for the DVDP2 basanite and DVDP2 hawaiite at 1,104°C

	Olivine		Clinopyroxene		Plagioclase	
	DVDP2 basanite	DVDP2 hawaiite	DVDP2 basanite	DVDP2 hawaiite	DVDP2 basanite	DVDP2 hawaiite
SiO_2	36.81–39.09	35.86–38.07	42.67–45.30	45.16–47.95	47.29–50.21	50.19–53.29
TiO_2			4.54–4.82	2.74–2.91		
Al_2O_3			7.91–8.39	5.28–5.60	28.80–30.59	28.17–29.91
FeO*[a]	20.70–21.98	22.50–23.90	6.46–6.86	7.23–7.67		
MgO	37.04–39.34	35.55–37.74	11.67–12.39	12.25–13.00		
CaO			21.45–22.77	21.08–22.39	12.98–13.79	11.55–12.27
Na_2O					2.70–4.04	3.30–4.94

Ranges for each represents the values including their standard deviations
[a]FeO* = Toral iron

from this and other one-atmosphere experimental studies with that of Sack et al. (1987) the effect of melt composition on this cotectic can be evaluated.

Kennedy et al. (1990) conducted one-atmosphere experiments from 1,191 to 1,119°C using a single bulk composition. Their data projected from the plagioclase apex of the normative olivine-diopside-nepheline-plagioclase tetrahedron to the olivine-diopside-nepheline base defines a cotectic slightly below but parallel to the one-atmosphere cotectic of Sack et al. (1987; Fig. 6). Temperature on this cotectic decreases from the olivine-diopside join towards the Ol-Di-Neph reaction point. Although this confirms the validity of one-atmosphere cotectic of Sack et al. (1987), a more comprehensive test to evaluate the effect of melt composition on the position of the olivine + high-Ca pyroxene + plagioclase + spinel cotectic would be to use one-atmosphere data from a suite of genetically related alkaline rocks. Data from this study (DVDP2 basanite and DVDP2 hawaiite) were projected from the plagioclase apex of Sack et al.'s (1987) pseudo-liquidus diagram (Fig. 6). Our data also define a cotectic with a trend towards the reaction point. The significant difference between our cotectic and those of Kennedy et al. (1990) is that their cotectic is located below the olivine + high-Ca pyroxene + plagioclase + spinel cotectic of Sack et al.'s (1987) whereas, the cotectic from our study is located slightly above and on the olivine + high-Ca pyroxene + plagioclase + spinel cotectic of Sack et al.'s (1987). Because the shifts in plotting coordinates of the cotectic are within the analytical uncertainties for these dry melts, we conclude that the position of the one-atmosphere cotectic as given by Sack et al. (1987) is composition independent to the first order.

Because natural hawaiite contains kaersutite, Mt Erebus hawaiite magma must have some water. An important issue to raise at this point is the effect of water on the position of the cotectic in the olivine-diopside-nepheline pseudoternary diagram. We do this by again referring to Fig. 6. We have plotted two additional compositions on this figure to demonstrate the effect of water. CSQ-3 is an alkali basalt, and SSC-1 is an olivine basalt. Their dry melt compositions are represented by an open triangle and an open circle, respectively. The triangle with a dot and the circle with a dot represent the same compositions with one weight percent water added at 100 bars. The dramatic shift in the positions of these two compositions compared to the compositions of the Mt. Erebus rocks and other alkaline rocks plotted in Fig. 6 indicate that Mt. Erebus magmas contain much less than one percent water. In addition, at 100 bars, complete crystallization of the CSQ-3 and SSC-1 compositions produced biotite, which has much more water than kaersutite. Therefore a magma from which kaersutite crystallizes must have less than one weight percent water. We can show this using the bulk composition of a basanite containing Ti-rich kaersutittic amphibole from the island of Tristan da Cunha in the South Atlantic (open star in Fig. 6). As our calculations with CSQ-3 and SSC-1 show, if an alkaline magma has water contents much less that one weight percent, its position in the normative olivine-diopside-nepheline diagram will not change significantly relative to the dry magma. We therefore conclude that even though the natural hawaiite from the Mt. Erebus has a small amount of kaersutite, our interpretation of its petrogenesis using the one

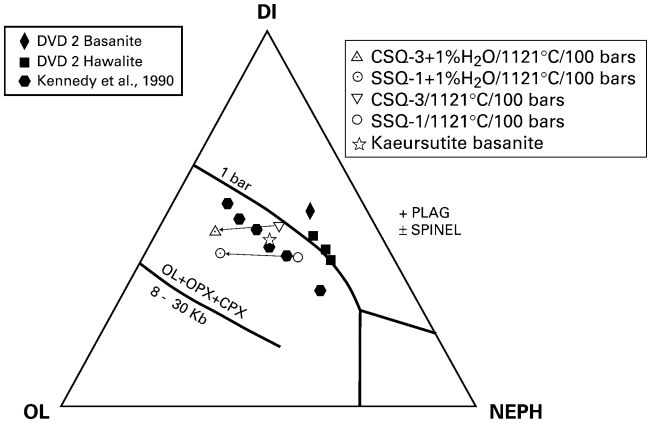

Fig. 6 Pseudo-liquidus phase diagram from Sack et al. (1987, Fig. 12) with cotectics of Kennedy et al. (1990) and DVDP2 basanite (1,104°C) and DVDP2 hawaiite (1,120–1,049°C) experimental glass data from this study

atmosphere anhydrous experimental data is nevertheless valid.

Finally, we endeavored to determine if the Ti-content of high-calcium pyroxenes could be used as a petrogenetic indicator. First, it was noted that multiple pyroxenes of differing Ti-contents were produced in our experiments on DVDP2 basanite at 1,138°C and on various alkalic lavas in experiments at 1,149°C by Sack and Carmichael (1984). These arrays of pyroxene compositions have average Ti-contents similar to those for low-Ti high-calcium pyroxenes coexisting with high-calcium pyroxenes in the simple system $CaMgSi_2O_6$–$CaMg_{1/2}Ti_{1/2}AlSiO_6$–$CaAl_2SiO_6$ at these temperatures (Fig. 2b). This observation appears to confirm the flat nature of the Gibbs free energy surface along the directions of the exchange vectors of interest (Sack and Ghiorso 1994b) and of a simple extrapolation of these gaps into the composition space defined by the pyroxenes of the Mt. Erebus lavas. Further support for this systematics is provided by the decrease of the average Ti-contents of the natural pyroxenes for the Mt. Erebus lavas in the sequence of DVDP2 basanite (0.114 ± 0.037), DVDP2 hawaiite (0.093 ± 0.020), 83415 Ne-hawaiite (0.079 ± 0.009), anorthoclase phonolite (0.060 ± 0.035 pfu; Fig. 2a). Pyroxenes in DVDP2 basanites have average Ti-contents appropriate to temperatures roughly in the range 1,170–1,070°C for low-Ti pyroxenes coexisting with high-Ti pyroxenes in the simple system $CaMgSi_2O_6$–$CaMg_{1/2}Ti_{1/2}AlSiO_6$–$CaAl_2SiO_6$. The experiments on DVDP2 basanites indicate that pyroxenes crystallize over a temperature range displaced downwards only 15 to 20°C, thus suggesting that the basanite pyroxenes were close to saturation with a high-Ti high-calcium pyroxene, the presence of a tiny amount of which might explain the high-Ti value of the pyroxene compositions determined by microprobe analysis. Likewise there is a similar close correspondence between the temperature inferred for pyroxenes from DVDP2 hawaiite and the liquidus temperature experimentally determined for this evolved lava, 1,104–1,120°C (Fig. 2a). Finally, there is a cluster of pyroxenes from the anorthoclase phonolite with an average Ti-content of 0.037 ± 0.011 pfu. The rest range from 0.07 to 0.13 pfu (Fig. 2b). MELTS (Ghioros and Sack 1995) predicts a high-Ca pyroxene with a Ti-content of 0.05 pfu at 900°C, which roughly corresponds to the cluster of low-Ti pyroxenes on Fig. 2b.

Figure 2a shows all the clinopyroxenes from the anorthoclase phonolite. The cluster of low-Ti, low-Al clinopyroxenes can be explained by equilibrium at about 900°C but other clinopyroxenes with higher-Ti, and higher-Al contents in anorthoclase phonolite must have a different origin. These pyroxenes would not form at this temperature because the activity of silica in the melt is not low enough. Thus, these pyroxenes must have a different origin than crystallizing from the anorthoclase phonolite melt. One possible explanation is that there are domains of low-Ti, low-Al and high-Ti and high-Al in these pyroxenes. That may explain the range in Ti and Al shown by these clinopyroxenes. Another possibility is that these clinopyroxenes have been incorporated into the anorthoclase magma from other sources. Future work on trace and REE of clinopyroxenes of the anorthoclase phonolites from the Mt. Erebus may shed more light on the origin of these clinopyroxenes.

Acknowledgements We would like to thank Dr. P. Kyle at New Mexico Institute of Mining and Technology for providing the samples for this study. We would also like to thank the Department of Earth and Atmospheric Studies of Purdue University for use of the Electron Microprobe and the Department of Geology at the University of Cincinnati for supporting this research. Finally we would like to thank two reviewers whose comments and suggestions greatly improved the manuscript.

References

Albee AL, Ray L (1970) Correction factors for election microprobe microanalysis of silicates, oxides, carbonates, phosphates, and sulfates. Anal Chem 42:1408–1414

Araña V, Martf J, Aparicio A, García-Cacho L, García-García R (1994) Magma mixing in alkaline magmas: an example from Tenerife, Canary Islands. Lithos 32:1–19

Aurisicchio C, Brotzu P, Morbidelli L, Piccirillo EM, Traversa G (1983) Basanite to peralkaline phonolite suite, quantitative crystal fractionation model (Nyambeni Range, East Kenya Plateau). N Jahrb Mineral Abh 148:113–140

Bence AE, Albee AL (1968) Experimental correction factors for the electron microanalysis of silicates, and oxides. J Geol 76:382–403

Brotzu P, Morbidelli L, Piccirillo EM, Traversa G (1983) The basanite to peralkaline phonolite suite of the Plio-Quaternary Nyambeni multicentre volcanic range (East Kenya Plateau). N Jahrb Mineral Abh 147:253–280

Camur MZ (1989) Experimental and numerical study of low pressure mineral-melt equilibria in alkaline lavas. PhD dissertation, Univ Cincinnati

Camur MZ, Kilinc AI (1995) Empirical solution model for alkalic to tholeiitic basic magmas. J Petrol 36:497–514

Gee LL, Sack RO (1988) Experimental petrology of melilite and nephelinites. J Petrol 29:1233–1255

Gerke TL (1995) Low pressure experiments with basanite, hawaiite, and phonolite from Mt. Erebus, Antarctica. PhD dissertation, Univ Cincinnati

Gerke TL, Kilinc AI (1993) Enrichment of SiO2 in rhyolites by fractional crystallization—an experimental-study of peraluminous granitic-rocks from the St. Francois Mountains, Missouri. Lithos 29:273–283

Ghiorso MS, Sack RO (1995) Chemical mass transfer in magmatic processes IV. A revised and internally consistent thermodynamic model for the interpolation and extrapolation of liquid–solid equlibria in magmatic systems at elevated temperatures and pressures. Contrib Mineral Petrol 193:196–212

Grove TL, Juster TC (1989) Experimental investigations of low-Ca pyroxene stability and olivine-pyroxene liquid equilibria at 1-atm in natural basaltic and andesitic liquids. Contrib Mineral Petrol 103:287–305

Grove TL, Gerlach DC, Sando TW (1982) Origin of Calc-alkaline series lavas at Medicine Lake Volcano by fractionation, assimilation and mixing. Contrib Mineral Petrol 80:160–182

Kennedy AK, Grove TL, Johnson RW (1990) Experimental and major element constraints on the evolution of lavas from Lihir Island, Papua New Guinea. Contrib Mineral Petrol 104:722–734

Kilinc AI, Gerke TL (2003) Compositional dependency of Fe–Mg exchange between olivine and melt. GSA Abs 35(6):72

Kilinc AI, Carmichael ISE, Rivers ML, Sack RO (1983) The ferric–ferrous ratio of nature silica liquids. Contrib Mineral Petrol 83:136–140

Kyle PR (1976) Geology, mineralogy, and geochemistry of the Late Cenozoic McMurdo Volcanic Group, Victoria Land, Antarctica. PhD thesis, Victoria University of Wellington

Kyle PR (1977) Mineralogy and glass chemistry of recent volcanic ejecta from Mt. Erebus, Ross Island, Antarctica. NZ J Geol Geophys 20:1123–1146

Kyle PR (1981) Mineralogy and geochemistry of a basanite to phonolite sequence at Hut Point Peninsula, Antarctica, based on core from dry valley drilling project drill holes 1, 2, 3. J Petrol 22:451–500

Kyle PR (1990) A.III. Erebus volcanic province. In: Le Masurier WE, Thomson JW (eds) Volcanoes of the Antarctic Plate and Southern Oceans. Antarctic Research Series 48: 81–88

Mahood GA, Baker DR (1986) Experimental constraints on depths of fractionation of mildly alkalic basalts and associated felsic rocks: Pantelleria, Strait of Sicily. Contrib Mineral Petrol 93:251–264

Moore JA (1986) Mineralogy, geochemistry, and petrology of lavas of Mt. Erebus, Antarctica. MS thesis, New Mexico Institute of Mining and Technology

Ringwood AE (1975) Composition and petrology of Earth's mantle. McGraw-Hill, New York, pp 618

Roedder PL, Emslie RF (1970) Olivine-liquid equilibrium. Contrib Mineral Petrol 29:275–289

Sack RO, Carmichael ISE (1984) Fe2+ ↔ Mg2+ and TiAl2 ↔ MgSi2 exchange reactions between clinopyroxenes and silicate melts. Contrib Mineral Petrol 85:103–115

Sack RO, Ghiorso MS (1994a) Thermodynamics of multicomponent pyroxenes: I. Formulation of a general model. Contrib Mineral Petrol 116:277–286

Sack RO, Ghiorso MS (1994b) Thermodynamic of multicomponent pyroxenes: III. Calibration of Fe+2(Mg)-1, TiAl2(MgSi2)-1, Ti(Fe+3)2(MgSi2)-1, AlFe+3(MgSi)-1, NaAl(CaMg)-1, and Ca(Mg)-1 exchange reactions between pyroxenes and silicate melts. Contrib Mineral Petrol 118:271–296

Sack RO, Walker D, Carmichael ISE (1987) Experimental petrology of alkalic lavas: constraints on cotectics of multiple saturation in natural basic liquids. Contrib Mineral Petrol 96:1–23

Smith AJ (1992) Experimental study of the Magdelena Obsidian: iron–magnesium exchange between olivine and high silica melt. MS thesis, University of Cincinnati

Thy P (1991) High and low pressure phase equilibria of a mildly alkalic lava from the 1965 Surtsey eruption: experimental results. Lithos 26:223–243

Ussler W, Glazner AF (1989) Phase-equilibria along a basalt-rhyolite mixing line—implications for the origin of calc-alkaline intermediate magmas. Contrib Mineral Petrol 101:232–244

Walker D, Shibata T, DeLong SE (1979) Abyssal tholeiites from the oceanographer fracture zone II. Phase equilibria and mixing. Contrib Mineral Petrol 70:111–125